July 2000 • NREL/CP-500-27551

Conference Paper

Maximizing Energy Capture of Fixed-Pitch Variable-Speed Wind Turbines

Kirk G. Pierce
Paul G. Migliore

Presented at the 38th AIAA Aerospace Sciences Meeting and Exhibit
Reno, Nevada
January 10–13, 2000

National Renewable Energy Laboratory

1617 Cole Boulevard
Golden, Colorado 80401-3393

NREL is a U.S. Department of Energy Laboratory
Operated by Midwest Research Institute • Battelle • Bechtel

Contract No. DE-AC36-99-GO10337

MAXIMIZING ENERGY CAPTURE OF FIXED-PITCH VARIABLE-SPEED WIND TURBINES

Kirk G. Pierce and Paul G. Migliore

National Renewable Energy Laboratory
1617 Cole Boulevard, Golden, CO 80401

ABSTRACT

Field tests of a variable-speed, stall-regulated wind turbine were conducted at a U.S. Department of Energy Laboratory. A variable-speed generating system, comprising a doubly-fed generator and series-resonant power converter, was installed on a 275-kW, downwind, two-blade wind turbine. Gearbox, generator, and converter efficiencies were measured in the laboratory so that rotor aerodynamic efficiency could be determined from field measurements of generator power. The turbine was operated at several discrete rotational speeds to develop power curves for use in formulating variable-speed control strategies. Test results for fixed-speed and variable-speed operation are presented along with discussion and comparison of the variable-speed control methodologies. Where possible, comparisons between fixed-speed and variable-speed operation are shown.

INTRODUCTION

In the last several years, there has been a dramatic increase in the number of variable-speed turbines deployed. By the end of this year, worldwide capacity of variable-speed turbines installed by Enercon will reach 1.4 GW and Enron will install more than 500 MW of its Z-750 series turbines in the U.S. alone [Migliore, 1999]. Information regarding the electrical characteristics, efficiency, and cost of these systems is now available to those having access to field-test data. Nevertheless, research continues on ways to improve the performance of variable-speed generating systems (VSGS), particularly as it relates to the undesirable electrical transients produced by power electronics. The U.S. Department of Energy's National Renewable Energy Laboratory (NREL) supports numerous projects involving VSGS components and subsystems. NREL's subcontract with Electronic Power Conditioning, Inc. (EPC) of Salem, Oregon, focused on the use of doubly-fed (wound-rotor) generators for variable-speed turbines. It is now generally accepted that this approach is the least expensive VSGS implementation because only the generator rotor current, which is typically 20%–30% of the rated current, must be conditioned by the power converter. In addition to reducing converter costs in this manner, EPC proposes the use of a soft-switching device. This approach allows higher switching frequencies and smaller voltage transients compared to traditional pulse-width-modulated (PWM) power converters. Extensive field tests of EPC's system were conducted at NREL's National Wind Technology Center (NWTC) during the 1998 and 1999 wind seasons.

After building and testing a proof-of-concept VSGS for Zond's prototype Z-46 turbine, EPC's primary objective in the NWTC tests was to move closer to a commercial prototype by demonstrating functionality, determining the converter rating (power) required to provide adequate control, measuring component efficiencies, reducing physical size, and determining cost. The field tests also provided a rare opportunity to accomplish other objectives, which included:

- measuring all drivetrain component efficiencies
- determining rotor power-coefficients at different Reynolds numbers
- measuring noise as a function of blade tip speed
- comparing power-rpm transients and dynamic loads to those in constant-speed operation
- developing various VSGS control methods, and
- developing advanced turbine control strategies.

Figure 1. AWT-26 wind turbine used in field tests

This last objective was aimed at improving upon Muljadi's variable-speed control strategy [Muljadi et al, 2000] and obtaining empirical data with which to examine the hypotheses of Mercer and Bossanyi [1996] regarding power regulation at wind speeds above rated. They concluded that "power quality," essentially the variation of the power about the rated value, is at least as good as constant-speed stall-regulated turbines, and the simulations indicated that the gearbox rating need not be any larger.

Development and testing of advanced control strategies is the focus of the present paper, although information is also presented on other aspects of the experiment. Complete details of the project are found in EPC's final NREL report [Weigand et al, 1999].

TURBINE DISCRIPTION

The host wind turbine for the EPC VSGS tests was the AWT-26 shown in Figure 1. It is a two-blade, teetering, downwind, free-yaw machine having a rotor diameter of 26 m. This 275-kW turbine was designed by R. Lynette and Associates of Seattle, Washington, and later commercialized with a 27-m diameter by Advanced Wind Turbines, Inc. (AWT) of San Raphael, California.

Variable-speed tests of the AWT-26 could have been performed using full power conditioning of its standard induction generator, but an important objective of the project was to investigate partial power-conditioning using the EPC soft-switching converter and a doubly-fed generator. Therefore, the standard drivetrain was replaced with a new gearbox, generator, and converter optimized for the AWT-26.

While this retrofit was being performed, we took the opportunity to reinforce the chassis and refurbish the teeter system in accordance with the manufacturer's recommendations. In addition, rotor blades were inspected and cleaned and the tip-vane aerodynamic brakes were serviced. Retrofit of the test turbine was completed with the installation of the power converter, new droop cables, fiber-optic signal conductors, and communications wiring between EPC's VSGS controller and AWT's supervisory controller. Details of the drivetrain design and laboratory tests are contained in Weigand et al [1999].

Drivetrain Retrofit

The standard AWT-26 gearbox with a ratio of 1:31.5 is the two-stage planetary PZBS-170, manufactured by Flender Corporation of Elgin, Illinois. Although the unit in the NREL turbine was serviceable, we installed a new gearbox having a ratio of 1:26.07 because it was more representative of an optimized gearbox/generator/converter that would be used commercially. This choice made the performance, cost, and efficiency of the drivetrain more germane to the planned cost-benefit analyses.

Selection of the lower gearbox ratio placed constraints on both maximum power (P_{max}) and rotor speed (rpm_{max}) for the experiment, because our safety protocol required that either the tip-vane aerodynamic brakes or the mechanical disk brakes, acting independently, should be capable of stopping the rotor in an emergency situation. With its standard 4-pole (1800-rpm) induction generator the constant-speed AWT-26 operates at a nominal rotor speed of 57.14 rpm. For any rotor power, the modified turbine, because of its lower gearbox ratio, experiences a higher torque at the high-speed mechanical brake than the standard turbine. Therefore, for variable-speed operation of the modified turbine, the input torque to the mechanical brake became a limiting factor. For the constant-speed generating system (CSGS), typical P_{max} and overspeed set-points are 300 kW and 63 rpm, respectively. But for the modified turbine, maximum power and rotor speed were set at 240 kW and 58 rpm, respectively, and the overspeed set-point as sensed by the EPC generator encoder was 61 rpm.

Design of the variable-speed drivetrain is a precise and restrictive effort requiring careful consideration of rotor characteristics, desired rpm range, component costs, component efficiencies, and mechanical restrictions. Calculations by AWT engineers suggested a useful rotor speed range of 30–62 rpm, which, in combination with the 1:26.07 gearbox ratio, resulted in a generator speed range of 780–1620 rpm. Taking these issues into consideration, including a restriction on frame size due to clearance requirements, EPC selected a 6-pole (1200-rpm) generator manufactured by Reuland Electric Company of Industry, California. Its stator and rotor current are 285 Amps and 120 Amps, respectively, and the rotor:stator winding ratio is 2.6:1.

EPC's unipolar series-resonant converter (USRC) is a bi-directional unit based on patented soft-switching power circuit topology. Because the main power switches are inverter-grade thyristors, it is possible to build this converter for high power levels (300–500 kVA at 480 VAC). It is characterized by good conversion efficiency and exceptional power quality, both on the grid and the load side.[*] While the

[*] Laboratory tests of the USRC [Weigand et al, 1999] showed good conversion efficiency and exceptional power quality. However, recent developments suggest the optimum doubly-fed VSGS might be a hybrid four-quadrant PWM converter with a standard hard-switched PWM bridge on the grid side and a parallel-resonant soft-switched bridge on the generator side.

operational mode (current-source, voltage-source, or voltage/frequency) on the load side can be selected for the particular application, control of the doubly-fed generator necessitates operating in the current-source mode. For the AWT-26, EPC fabricated a 480 VAC converter having a one-minute rating of 110 kVA, an output current of 130 Amps, and an overload capacity of 150%. It is important to note that the determination of an appropriate overload capacity was an important objective of the field tests, because the ability of the VSGS to restrain P_{max} was not known *a priori*.

Variable-speed operation of the AWT-26 was accomplished through the VSGS controller developed by EPC. Its functions were: (1) real-time control of the doubly-fed generator by means of the USRC, (2) real-time VSGS protection through continuous monitoring of system fault inputs, (3) interface with the operator, and (4) interface with the AWT-26 supervisory controller. This last function was implemented by simple enable-fault communications. The interface consists of one line from the AWT-26 controller requesting a VSGS start-up upon contact closure (or shutdown upon contact opening), a second line from the VSGS controller communicating a VSGS fault to the AWT-26 controller upon contact opening, and a third line from the VSGS controller communicating that the doubly-fed generator has been synchronized to the utility grid upon contact closure. The interface was implemented so that interruption of any of these lines is interpreted as a command to shut down the turbine.

Component Efficiencies

Because an important objective of these experiments was to understand the relationship between rotor power, generator power, and rpm, we resolved to measure the efficiencies of all drivetrain components for the baseline AWT-26 and the modified variable-speed turbine [Weigand et al, 1999]. Gearbox efficiency tests over a broad range of temperatures and rotational speeds were conducted at The Gearworks of Seattle, Washington. The standard AWT-26 (U.S. Motors) induction generator, the Reuland doubly-fed generator, and the EPC power converter were tested at EPC's facilities in Corvallis, Oregon. The component efficiency data were invaluable in devising the power-rpm trajectories for variable-speed control strategies and deducing rotor-power (and power coefficient) curves from measured generator-power curves.

FIELD TESTS

We operated the turbine at several discrete rotor speeds in the rpm-range we intended to investigate. Our purpose was to characterize the system dynamics and determine rotational frequencies to be avoided during variable-speed operation. These tests, the data acquisition system, and the test sequence are described below.

Dynamic Characterization Tests

We anticipated operating the EPC/AWT-26 variable-speed turbine over a wide range of rotational speeds. To ensure that we did not encounter any potentially damaging vibrations, dynamic characterization tests were performed [Larwood, 1998]. These tests indicated potential resonances at rotational speeds of 32, 38, 48, 52, and 56 rpm. Some of the vibrational frequencies were at higher harmonics of the blade passing frequency and did not prove problematic. Nevertheless, the VSGS controller was programmed to pass through all these rotational speeds without dwelling. Rotational speeds of 32 rpm and 56 rpm indicated potential resonances at vibrational frequencies equivalent to two-cycles per revolution. Unfortunately, it was necessary to operate at 32 rpm to characterize the power curve at a low Reynolds number, an important test objective. At this rotational speed, a dramatic coupling of nacelle-yaw and tower-lateral motion at low wind speeds caused great apprehension in the test engineers. Therefore, once the critical data were obtained, discrete rpm tests were run at more tranquil rotor speeds.

Data Acquisition Systems

Two data acquisition systems were used to collect test information. A low-frequency system recorded one-minute averages of important power-performance and meteorological data. A high-frequency system recorded power-performance transients and turbine structural responses for use in evaluating variable-speed control strategies and making comparisons to constant-speed operation. The data acquisition systems were independent of each other.

Low-frequency data were acquired using a Campbell Scientific 21X data logger mounted on the meteorological tower approximately two rotor diameters upstream of the turbine in the prevailing wind direction. There were no obstructions in this direction for 18.75 rotor diameters. The data logger sampled at 1 Hz and recorded one-minute averages with statistics of all data. Information was stored on a Campbell Scientific M1 module and downloaded to a programmable computer on a weekly basis. The recorded data included atmospheric temperature and pressure, generator speed, power output, gearbox temperature, and hub-height wind speed and direction.

High-frequency data were acquired using an Analog Devices 5B01 backplane with signal conditioning devices. A National Instruments DAQCard-AI-

16XE-50, installed in a laptop computer PCMCIA slot, was connected to the 5B01 backplane for analog-to-digital conversion of the signals. Data were sampled at 20 Hz and stored in files of ten-minute length. The sampling rate of 20 Hz was more than twice the Nyquist frequency for all signals of interest. The data recorded were hub-height wind speed, generator speed, power output, and nacelle acceleration in two orthogonal directions. No rotating frame measurements were recorded because of the limited scope of this study, the primary objective of which was the evaluation of the converter and control methodologies for fixed-pitch stall-regulated turbines.

Test Sequence

Before we began variable-speed testing of the AWT-26, we determined its characteristics with the standard constant-speed induction generator. Although NREL and AWT possessed data from previous tests, we wanted to obtain a baseline power curve for the exact turbine at the same site used to obtain variable-speed test data. Furthermore, because drivetrain component efficiencies were known for the NWTC turbine, it would be possible to deduce rotor power coefficients from generator electrical power measurements. Approximately 140 hours of test data were collected for the baseline turbine operating at its nominal 57 rpm. After filtering and binning the data in the manner described below, a power curve was constructed from approximately 57 hours of these data.

In preparation for testing the variable-speed control strategies, we obtained power curves for the EPC AWT-26 variable-speed turbine at two discrete rotor speeds. Our original intent was to obtain a power curve at 55 rpm for comparison to the baseline power curve. However, we opted for a more conservative test at 50 rpm because we were testing a new system with unproven characteristics. The dynamic characterization tests indicated placid operation at this rotor speed, and we were quite confident that the EPC power converter and the AWT-26 brake systems would maintain safe conditions. For this test, we collected approximately 53 hours of test data from which a power curve was constructed of approximately 49 hours of filtered data.

Another power curve was obtained for the EPC/ AWT-26 variable-speed turbine at 32 rpm. Although we preferred not to operate at this rotor speed, which was predicted to be dynamically active, we thought it important to learn of any important differences in optimum power coefficient or tip-speed ratio for low rotor speeds. The availability of the variable-speed turbine provided a rare opportunity to observe Reynolds number effects empirically, rather than to treat them hypothetically. For the 32-rpm case, we collected approximately 30 hours of test data, from which a power curve was constructed of approximately 20 hours of filtered data. Although we wanted to obtain considerably more data, it was difficult to test at this rpm. Furthermore, the wind-speed range of interest (4–12 m/s) at 32 rpm is much narrower than for the 50-rpm case (5–20 m/s) or the 57-rpm case (5–24 m/s). Considering the objectives of the tests, there was not much interest in obtaining data beyond these wind speeds, where the blades are in deep stall.

Because the ability of the VSGS to constrain power and rotor speed was unproven, we chose a conservative approach for the first variable-speed tests. The algorithm used, called the "*soft-stall*" method, is described in detail in Muljadi et al [2000]. Approximately 32 hours of data were collected in these tests, from which 22 hours of filtered data were used to construct the power curve.

A second, more aggressive strategy is the principal subject of this paper. When we gained confidence in the ability of the VSGS to constrain power and rotor speed, we enlarged the operating region of the turbine near rated power. The purpose was to replicate a variable-speed, variable-pitch power curve using the variable-speed, stall-regulated (fixed-pitch) turbine and "*active-control*" methods. Approximately 40 hours of data were collected in these tests, from which 24 hours of filtered data were used to construct the power curve.

In addition to the power curves described above, some high-frequency (20 Hz) test data were obtained for wind speed, power, generator speed, and nacelle accelerations. These data formed the basis for limited dynamic analyses of variable-speed operation of the AWT-26 in comparison to the constant-speed baseline turbine.

Data Reduction

For developing power curves, the one-minute-average wind speed, rotor speed, and generator power were downloaded from the Campbell 21X data-logger, along with atmospheric temperature and pressure, and turbine status. These data were "filtered" by removing points that did not meet the acceptance criteria, which were:

- wind directions from 165^{o} to 332^{o}
- turbine not off-line due to grid or turbine faults
- sensors and data system functioning properly
- turbine not in start-up, manual, standby, or shutdown.

The filtered data were normalized to a site-average air density of 1.0 kg/m^3, then sorted and tabulated in wind-speed bins of 0.5 m/s (4.75–5.25 m/s, 5.25–5.75 m/s, and so forth). Typical data presentation is a scatter-plot of power versus wind speed (or rpm) and superimposed

power curve of median wind speed versus mean generator power for the data in the bins.

A similar approach was used to develop *Cp*-TSR curves, where the power coefficient (*Cp*) and tip-speed ratio (TSR) were calculated for each one-minute average data point, then normalized, binned, and plotted. Because our interest was in rotor *Cp*, the measured generator power was converted to rotor power by correcting for gearbox, generator, and converter efficiencies (for the VSGS) measured in the laboratory.

High-frequency power data were smoothed and filtered to remove data spikes caused by the self-powered OSI power transducer. The post-processing software GPP [Buhl and Weaver, 1999] was used to calculate rainflow cycle-counts for comparing operating methods. Time-series plots of the data are also presented.

CONTROL METHOD

The *active-control* method attempts to maximize the energy capture of a fixed-pitch variable-speed turbine having constraints on its maximum rpm and power. To maximize energy capture, it is desirable to operate at maximum power coefficient (Cp_{max}) over the broadest possible rpm range. However, at some wind speed the turbine will reach its maximum allowable rotor speed (rpm_{max}), at which point the rotor speed must be constrained. The turbine is then operated at rpm_{max} up to the wind speed at which (P_{max}) is reached. Thereafter, power is constrained through a reduction of rotor speed, thereby stalling the rotor in high winds. This approach provides the maximum possible energy capture within the rpm and power constraints. Figure 2 illustrates the *active-control* approach in comparison to the more conservative *soft-stall* approach [Muljadi et al, 2000]. The differences between the two methods are the range of Cp_{max} operation and the method for limiting rotor speed.

In the *soft-stall* method, rotor speed is not actively controlled. Power and rpm are constrained through a process of requesting more power than the turbine is capable of producing. In the stall region, rotor speed is less than the allowed maximum, and rated power occurs only at one wind speed. An advantage of the *soft-stall* method is that it does not require active control. Only a requested torque or power specified as a function of rotor speed is needed.

To improve energy capture, the range of Cp_{max} operation must be extended and upon reaching rpm_{max}, rotor speed must be regulated through active control. For the current study, a proportional and integral (PI) algorithm was used to control rotor speed to the desired set-point value in the rpm_{max} region. In the Cp_{max} region, a

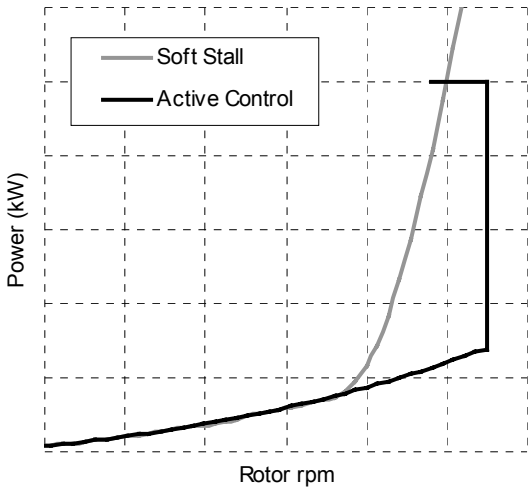

Figure 2. Comparison of variable-speed fixed-pitch control methods

torque-rpm table is used. The difficulties in controlling this system are in the transitions between the regions and in constraining power to P_{max}. In the transition from Cp_{max}- to rpm_{max}-operation, it is necessary to decelerate the rotor if its speed is rapidly approaching rpm_{max}. To achieve this, the PI algorithm and the Cp_{max} torque procedure should run concurrently, and the maximum of the two dictated torque values should be selected as the current value. Increasing the proportional gain will allow the turbine to approach the set-point value without overshooting. Regulation of power in high winds is more difficult. Because rpm_{max} control was already implemented, P_{max} control was formulated to use the same system through the adjustment of the rpm_{max} set-point value.

The control system schematic is shown in Figure 3. Here, K_I is the integral gain and K_P is the proportional gain. $T(\omega)$ is the torque as a function of rotor speed required to track Cp_{max}. The MAX block selects the maximum torque obtained from the torque-speed curve and the PI system. The rpm set-point is determined as a function of the output power (P) and rotor speed (ω) shown as block $f(P,\omega)$. Wind-up of the integrator must also be prevented.

To determine the rpm set-point, we begin with the aerodynamic torque, neglecting losses, given by:

$$T_{aero} = I\dot{\omega} + T_{gen} \qquad (1)$$

T_{aero} is the aerodynamic torque, T_{gen} is the generator torque referenced to the low speed shaft, and I is the inertia of the rotating system. $\dot{\omega}$ is estimated by differencing the measured rotor speed. This estimate of the aerodynamic torque is low-pass filtered to reduce noise and rapid signal fluctuations. Using the low-pass-

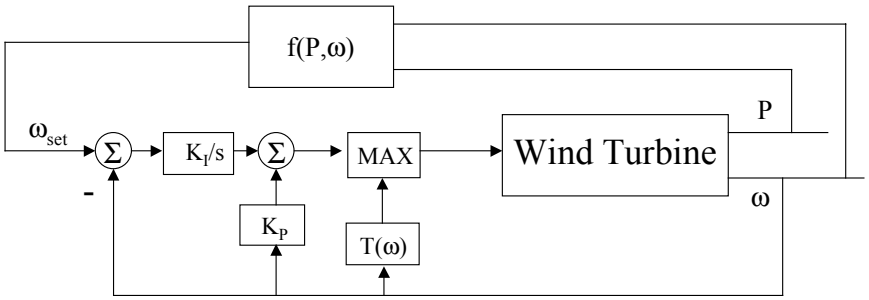

Figure 3. Schematic of *active-control* system

filtered value of the estimated aerodynamic torque, the rpm set-point is then determined from:

$$rpm_{set-point} = \frac{P_{desired}}{filter(T_{aero})}\frac{30}{\pi} \qquad (2)$$

The upper value of the rpm set-point is limited to rpm_{max}. The estimate of aerodynamic torque is used in the control to avoid the possibility of continually extracting kinetic energy from the rotating system to maintain rated power, thereby slowing the rotational speed excessively.

A previously-developed ADAMS® model of the turbine [Muljadi et al, 2000] was used for design of the control system, and final tuning of control parameters was done on the operating turbine.

RESULTS AND DISCUSSION

Constant-Speed Tests

Discrete-speed tests were performed on the VSGS for rotor speeds of 32 rpm and 50 rpm. Data were also available for the original CSGS operating at 57 rpm. Power curves for these three cases are shown in Figure 4, which illustrates, as expected, that maximum power increases significantly with increasing rotor speed.

Using the turbine (generator) power output measured in the field tests and the drivetrain component efficiencies measured in the laboratory tests, rotor *Cp* curves were deduced for each of the configurations of Figure 4. These rotor *Cp*-TSR curves are shown in Figure 5. The reduction in maximum *Cp* and optimum TSR at lower rpm is largely attributable to Reynolds number effects.

The Reynolds number at 75% of the blade span is approximately 1.6M at 32 rpm, 2.5M at 50 rpm, and 2.8M at 57 rpm, varying somewhat with wind speed. For the S809 airfoil [Somers, 1997], which is the primary airfoil used on the test blade, the lift characteristics are largely independent of Reynolds numbers. Drag characteristics, however, are sensitive to Reynolds numbers, with lower drag for higher Reynolds numbers. This results in a lift-to-drag ratio (L/D) at Re = 2.5M that is approximately 20% higher than at Re = 1.5M over the linear range of the lift curve, as shown in Figure 6. Also, the maximum L/D is lower for Re = 1.5M than for 2.5M, and it occurs at a higher angle of

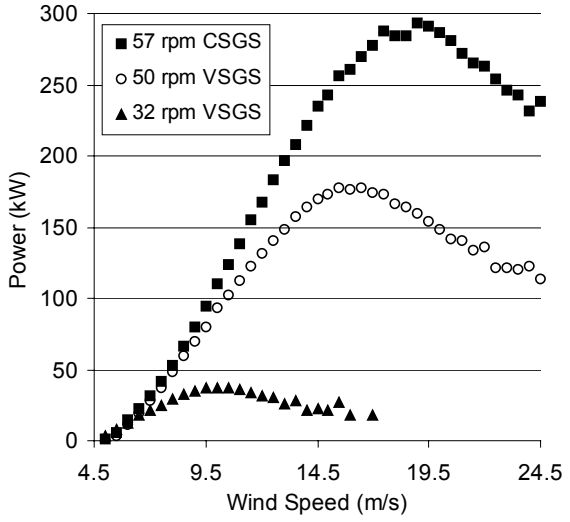

Figure 4. Measured power curves

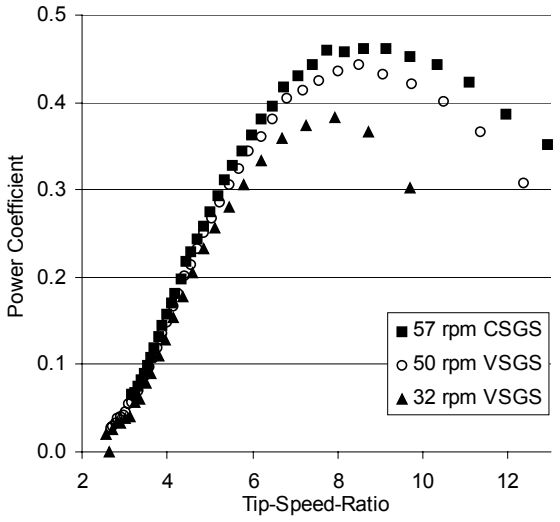

Figure 5. Rotor aerodynamic power coefficients

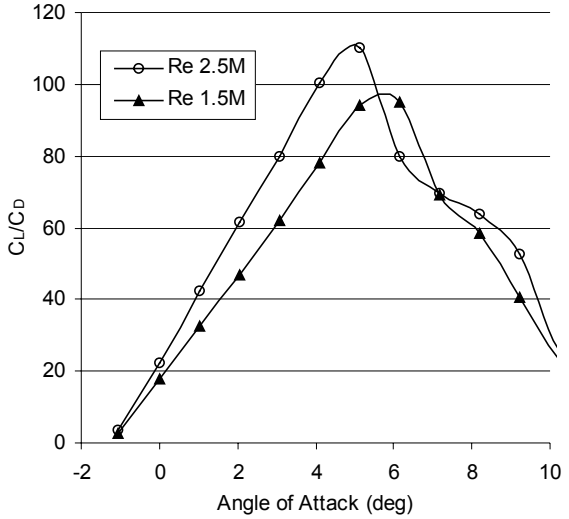

Figure 6. Lift-to-drag ratio for the S809 airfoil for two Reynolds numbers in the clean condition

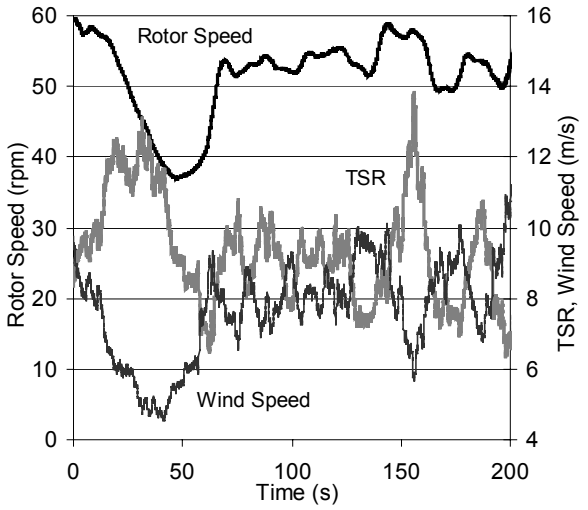

Figure 7. Time series of variable-speed operation

attack. Because of the strong dependence of *Cp* on L/D, maximum *Cp* is reduced and it occurs at a lower TSR (higher angle of attack) for lower rotor speeds. This is in accordance with the data of Figure 5.

The small difference in Reynolds number between 50 rpm and 57 rpm may not account for all the difference in the *Cp* curve. Other possibilities include unknown three-dimensional aerodynamic effects, differences in blade roughness, and errors in measuring or applying drivetrain component efficiencies. Differences between the 50-rpm and 32-rpm curves are not due to blade roughness, as those tests were performed concurrently. For a given wind speed, the turbine may have been operated at both rotor speeds to obtain desired power-curve data.

Variable-Speed Tests

Several important aspects of operation in the Cp_{max} region are illustrated in Figure 7, a time-series plot of important variables. In the first 40 seconds the rotor speed follows the decline in wind speed, but with a time lag of several seconds. As a result, the TSR increases substantially to non-optimum values. Between 60 seconds and 120 seconds, where wind-speed fluctuations are moderate, TSR variations are also moderate. The sudden drop in wind speed at 150 seconds again results in a lag in rotor speed and TSR tracking. This sequence illustrates that the AWT-26 does not effectively track the changing wind speed. The turbine was initially designed for constant-speed stall-regulated operation at a fairly high tip-speed ratio. The high design TSR adversely affects the turbine time constant and variable-speed tracking performance [Pierce, 1999]. Tracking a high TSR requires a greater change in rpm, and a greater change in kinetic energy, for a given change in wind speed. Another factor contributing to poor tracking during the decreasing wind segments is the slower turbine time constant for low winds.

Operation at high TSR also limits the range of wind speeds for Cp_{max} operation. The range of rotor speeds chosen for variable-speed operation of the turbine was between 32 rpm and 58 rpm. Tracking the optimum TSR = 9 at these rotor speeds results in a range of wind speeds between 5 m/s (cut-in) and 8.8 m/s. The upper wind speed for Cp_{max} operation corresponds to less than one-third of the rated power, resulting in a wide range of wind speeds where the rpm_{max} limit governs operation of the turbine. With the limitations noted above, comparing energy capture for fixed-speed and variable-speed operation of the AWT-26 is not meaningful. Instead, our emphasis is on the fact that the control methods used are applicable to fixed-pitch turbines properly designed for variable-speed operation.

The trajectory for Cp_{max} operation was chosen so that the turbine tracked the maximum aerodynamic *Cp* (determined in CSGS tests) by following the standard $k\omega^2$ relation[†]. The power-rpm schedule for this region was determined from the aerodynamic power by subtracting measured gearbox, generator, and converter losses. In hindsight, to maximize energy capture, one should *first* account for the rotor, generator, gearbox, and converter efficiencies *and then* determine the rpm for maximum power output at a given wind speed. The resulting

[†] It can be shown that the torque demand for operation at a specific Cp-TSR combination is given by $T = k\omega^2$, where *k* is a function of known constants.

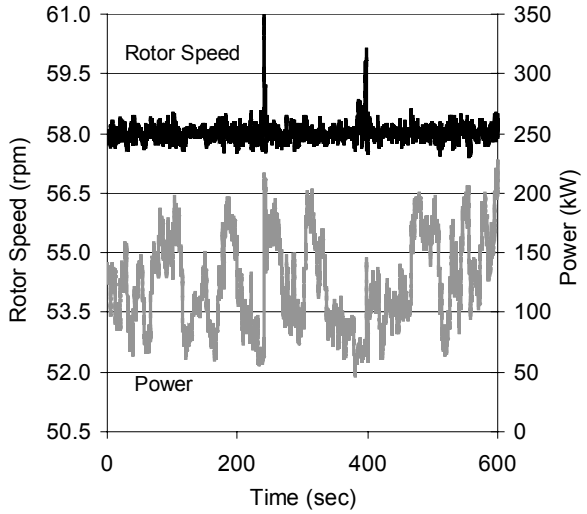

Figure 8. Time series of rpm-regulation for the *active-control* method

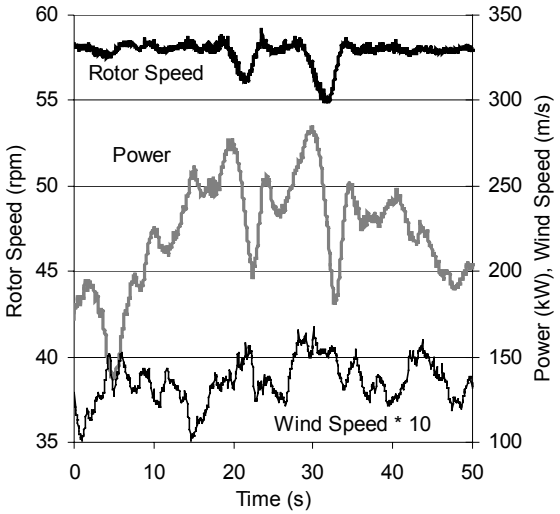

Figure 9. Time series of power regulation for the *active-control* method

power-rpm schedule, however, would maximize energy capture only for steady-state operation. In varying winds, the torque-rpm schedule affects the turbine's dynamic response. Therefore, some deviation from the steady-state optimal solution is likely to result in greater energy capture [Freris, 1990].

The ability of the *active-control* method to constrain rotor speed to the desired value of rpm_{max} is illustrated in Figure 8. The rpm trace clearly shows some anomalies, either in the algorithm or the software, which could be improved. But in general, the speed is well-regulated for a wide range of output power. Inspection of the data shows that the speed may be too well-regulated, because 2-P oscillations are evident. By observation of available data, it was seen that variation of rotor speed during rpm_{max} regulation is nearly the same as for constant-speed operation of the AWT-26. Therefore, it is probably desirable to adjust the system gains to allow greater variation in rotor speed during rpm_{max} regulation, thereby softening the drivetrain response and reducing the 2-P oscillations.

Unfortunately, very few test data were obtained for high wind speeds. A short time-series illustrating P_{max} regulation is shown in Figure 9. As the power output exceeds the set-point maximum of 240 kW, at a wind speed of approximately 14 m/s, rotor speed is reduced. However, there is some overshoot in the control as evidenced by the reduction in power substantially below the set-point value. Additional tuning of the control parameters should improve this response.

Figure 10 is a plot of one-minute averages of power-rpm data for the two variable-speed control strategies. Although some scattering of data is to be expected, particularly near transition rotor speeds, both methods have

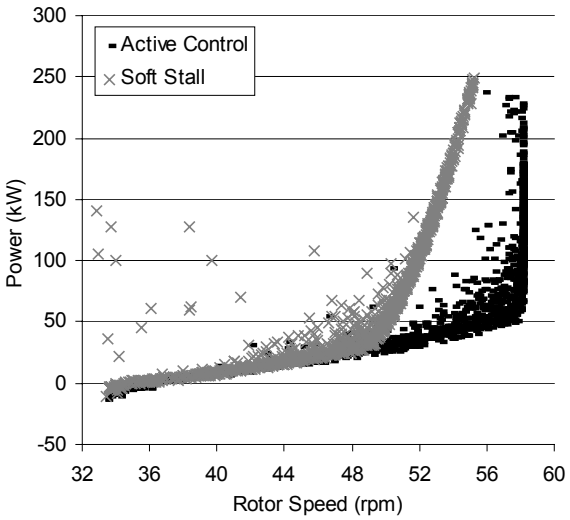

Figure 10. One-minute averages of power-rpm for the two variable-speed control methods

the structure of their desired power-rpm curves shown in Figure 2. *Active control* extends the Cp_{max} region and regulates rpm_{max} very well. Because there are very few data near P_{max} for the *active-control* method, definite conclusions can not be drawn about the effectiveness of the control in this region. However, observation by test engineers during turbulent winds above 15 m/s showed very few short-term (one-second) excursions above the P_{max} set-point value.

Power curves of filtered and binned test data for the two control methods are shown in Figure 11. *Active control* has the desired effect of increasing power output in medium and high wind speeds as compared to the *soft-stall* strategy. The two methods are equivalent in the Cp_{max} region of the *soft-stall* controller.

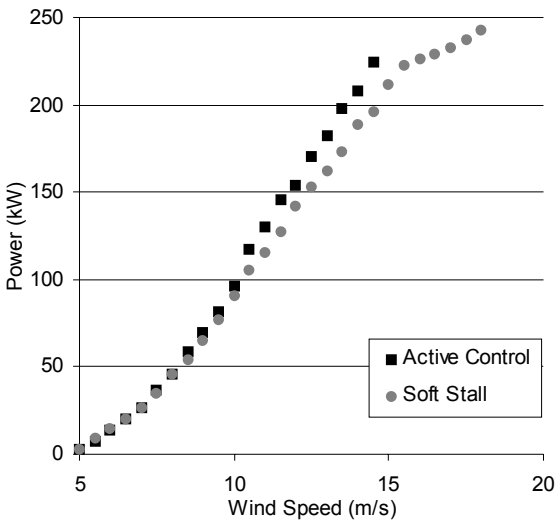

Figure 11. Filtered and binned power curves for the two variable-speed control methods

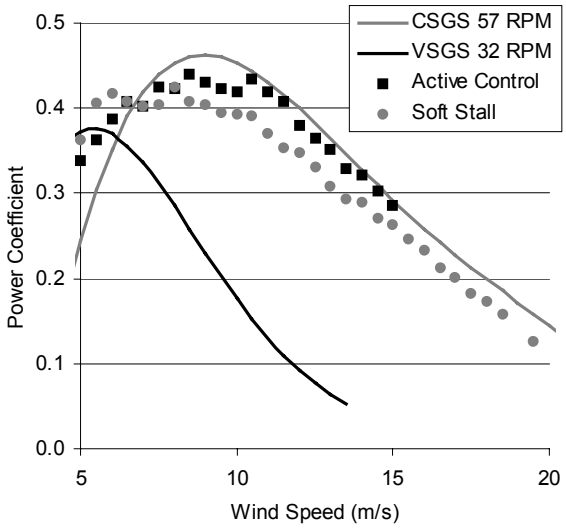

Figure 12. Rotor power coefficients for two discrete rotor speeds and the two variable-speed control methods

Comparison of Constant- and Variable-Speed Operation

Power-coefficient plots for two discrete rotor speeds and the two variable-speed methods are compared in Figure 12. The solid-line curve-fits to the data are used for clarity. *Cp* is plotted against wind speed rather than the typical *Cp*-TSR to better depict turbine operation. A variable-speed turbine operating at a rotor speed that exceeds the optimum TSR will decelerate as kinetic energy is extracted from the rotor. Power output is momentarily increased, not because of wind input, but because the kinetic energy of the rotor is being drained. This results in over-prediction of the C_p for high TSR, and under-prediction for low TSR, unless adjustments are made for the effects of rotor kinetic energy. However, when plotted as a function of wind speed the rotor is as likely to be accelerating as decelerating, resulting in a more accurate representation of the turbine operation.

Data for the two variable-speed control methods fall between the two fixed-speed curves, except at very low wind speeds. Figure 11 shows that power output of the two methods is virtually identical at low wind speeds, but the extreme sensitivity of *Cp* calculations to measured wind speed results in erratic plots of *Cp* data.

In winds above 11 m/s, data for the *soft-stall* control show a pattern similar to, but at a lower power than, the 57-rpm CSGS curve. Reference to Figures 10 and 11 shows that at those wind speeds the rotor operates in a narrow range between 53 rpm and 55 rpm.

In winds above 11 m/s, data for the *active-control* method are almost coincident with the 57-rpm CSGS curve. This is an encouraging result, because after adjusting for the slip of the CSGS generator, the rotor speeds are almost identical (58 rpm).

One result we wished to obtain from the field tests was a determination of the power-converter capacity needed to control the variable-speed stall-regulated turbine. For the 57-rpm CSGS, the maximum one-second average power seen in the data was 458 kW, which is 67% more than the rated power of 275 kW. For the *active-control* method, the maximum one-second average power seen in the data was 323 kW, which is 35% more than the set-point value of 240 kW. Although this is a considerable improvement, additional testing and control-parameter tuning would be needed to determine the required power converter capacity. An additional influence on the required converter capacity is the rotor inertia, which affects the transient loads associated with decelerating, and stalling the rotor [Mercer and Bossyani, 1996].

Also of interest are the effects of variable-speed operation on the drivetrain-components and tower fatigue-loads due to operation near resonant frequencies. Figure 13 is a plot of rainflow cycle-counts of drivetrain torque for Cp_{max} operation compared to discrete-speed operation at 58 rpm. For the variable-speed case, the mean wind speed was 6.2 m/s and the turbulence intensity was 15%. For the constant-speed case, the mean wind speed was 6.8 m/s and the turbulence intensity was 14%. The low-frequency, high-amplitude cycles have been reduced as a result of variable-speed operation.

Figure 14 is a plot of rainflow cycle-counts of nacelle acceleration in two orthogonal directions for the same data sets shown in Figure 13. In this case, the low-

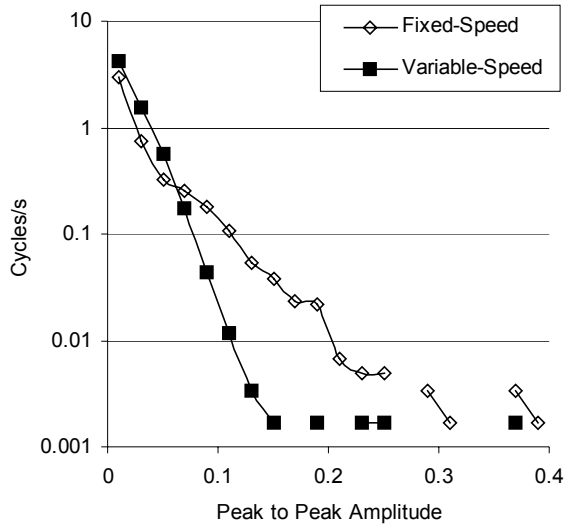

Figure 13. Rainflow cycle-counts of drivetrain torque for variable-speed and fixed-speed operation

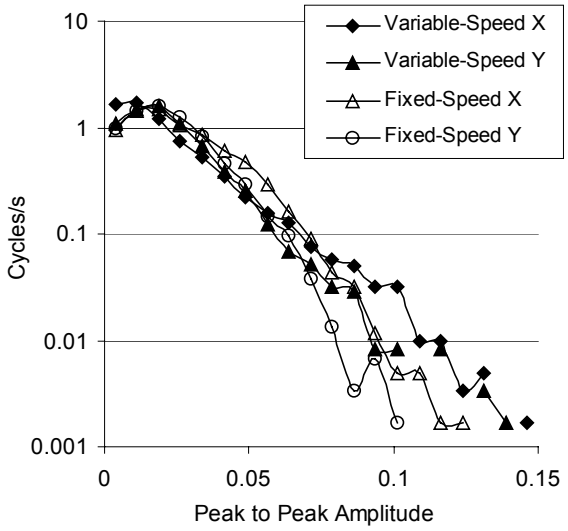

Figure 14. Rainflow cycle-counts of nacelle acceleration for variable-speed and fixed-speed operation

frequency, high-amplitude cycles have been increased as a result of variable-speed operation.

In the region of rpm_{max}-regulation, there should be little difference in structural loading between the *active-control* method and the constant-speed turbine. Transition from Cp_{max} operation to rpm_{max}-regulation may, however, result in increased torque cycles from decelerating the rotor. Insufficient data are available to assess these structural-loading effects.

CONCLUSIONS

Field tests of a variable-speed stall-regulated wind turbine were conducted at the NWTC. Data were obtained for the turbine operating at several discrete rotor speeds and for two variable-speed control strategies. Power coefficients for the rotor were deduced by correcting the turbine output (generator) power for drivetrain component losses measured in the laboratory. Some information was also obtained for the structural response of the different operating modes. The following conclusions are drawn from the field results and other supporting activities.

- Maximum *Cp* and the TSR at which it occurs show a strong dependency upon rotor speed. This is attributed primarily to Reynolds number effects, although there may be other contributing factors.
- The *active-control* method permits tracking of optimum TSR (peak *Cp*) while constraining maximum rotor speed and power to pre-set values. Excellent regulation of rpm_{max} was demonstrated, but insufficient data were obtained to conclusively demonstrate P_{max} constraint.
- Variable-speed operation at Cp_{max} decreased drivetrain cyclic-loading and increased tower fatigue-loading in comparison to constant-speed operation.
- Although the *active-control* method is immature, the preliminary results are promising. Additional testing, with the ability to tune the control parameters, is needed to determine the capability of the algorithm and the required converter capacity.
- Simulation results, observations of test engineers, and preliminary test results indicate that a properly designed VSGS is capable of mimicking the power curve of a variable-speed pitch-regulated turbine.
- The AWT-26 is not well-suited for variable-speed operation. This highlights the need to consider influential design parameters, such as TSR, rotor inertia, Reynolds number effects, and component efficiencies when optimizing variable speed turbines.

ACKNOWLEDGMENTS

The research and development activity reported herein was supported by the U.S. Department of Energy through a subcontract awarded by NREL. Many people were involved in the design, fabrication, and testing of the VSGS. The authors wish to express particular appreciation to Gregory Heine of the University of Colorado College of Engineering and Applied Sciences, Claus Weigand and Ashok Ramachadran of EPC, Timothy McCoy and Dayton Griffin of Kamzin Technology, Inc. (formerly Advanced Wind Turbines, Inc.), consultant Gene Quandt for assistance with data

analysis, and NREL test engineers Brian Gregory and Scott Larwood.

REFERENCES

Buhl, M.L., and Weaver, N.L., *GPP Version 6 Users Guide*, NREL/TP-442-5225, Golden CO, National Renewable Energy Laboratory, 1999.

Freris, L.L., *Wind Energy Conversion Systems*, Prentice Hall International, Hertfordshire, UK, 1990.

Larwood, S., *Dynamic Characterization of the AWT-26 Turbine for Variable Speed Operation*, NREL/TP-500-24919, Golden CO, National Renewable Energy Laboratory, July 1998.

Mercer, A., and Bossanyi, E., *Stall Regulation of Variable Speed HAWTS*, Proceedings of the 1996 European Union Wind Energy conference, Goteborg, Sweden, May 1996.

Migliore, P., Personal notes, European Wind Energy Conference and Exhibition, Nice, France, March 1999.

Muljadi, E., Pierce, K., and Migliore, P., *A Conservative Control Strategy for Variable-Speed Stall-Regulated Wind Turbines*, A Collection of the ASME Wind Energy Symposium Technical Papers at the 38th Aerospace Sciences Meeting and Exhibit, Reno, NV, January 2000, and NREL CP-500-26929, Golden, CO, National Renewable Energy Laboratory, October 1999.

Pierce, K., *Control Method for Improved Energy Capture Below Rated Power*, 3rd ASME/JSME Joint Fluid Engineering Conference, San Francisco, CA, June 1999.

Somers, D.M, *Design and Experimental Results for the S809 Airfoil*, Work performed by Airfoils, Inc., State College, PA, NREL/SR-440-6918, Golden, CO, National Renewable Energy Laboratory, January, 1997.

Weigand, C., Lauw, H., and Marckx, D., *Variable-Speed Generation Subsystem Using the Doubly-Fed Generator*, NREL SR-500-27066, Golden, CO, National Renewable Energy Laboratory, October 1999.